Egg White Sulfhydryl Oxidase: Kinetic Mechanism of the Catalysis of Disulfide Bond Formation†

Karen L. Hoober and Colin Thorpe*

Department of Chemistry and Biochemistry, University of Delaware, Newark, Delaware 19716

Received August 26, 1998; Revised Manuscript Received January 20, 1999

ABSTRACT: The flavin-dependent sulfhydryl oxidase from chicken egg white catalyzes the oxidation of sulfhydryl groups to disulfides with reduction of oxygen to hydrogen peroxide. The oxidase contains FAD and a redox-active cystine bridge and accepts a total of 4 electrons per active site. Dithiothreitol (DTT; the best low molecular weight substrate known) reduces the enzyme disulfide bridge with a limiting rate of 502/s at 4 °C, pH 7.5, yielding a thiolate-to-flavin charge-transfer complex. Further reduction to EH_4 is limited by the slow internal transfer of reducing equivalents from enzyme dithiol to oxidized flavin (3.3/s). In the oxidative half of catalysis, oxygen rapidly converts EH_4 to EH_2, but E_{ox} appearance is limited by the slow internal redox equilibration. During overall turnover with DTT, the thiolate-to-flavin charge-transfer complex accumulates with an apparent extinction coefficient of 4.9 mM^{-1} cm^{-1} at 560 nm. In contrast, glutathione (GSH) is a much slower reductant of the oxidase to the EH_2 level and shows a k_{cat}/K_m 100-fold smaller than DTT. Full reduction of EH_2 by GSH shows a limiting rate of 3.6/s at 4 °C comparable to that seen with DTT. Reduced RNase is an excellent substrate of the enzyme, with k_{cat}/K_m per thiol some 1000- and 10-fold better than GSH and DTT, respectively. Enzyme-monitored steady-state turnover shows that RNase is a facile reductant of the oxidase to the EH_2 state. This work demonstrates the basic similarity in the mechanism of turnover between all of these three substrates. A physiological role for sulfhydryl oxidase in the formation of disulfide bonds in secreted proteins is discussed.

Flavin-dependent sulfhydryl oxidases catalyze the oxidation of thiol groups to disulfides with the reduction of oxygen to hydrogen peroxide:

$$2RSH + O_2 \rightarrow RS{-}SR + H_2O_2$$

Enzymes isolated from rat seminal vesicles (*1*) *Aspergillus niger* (*2*) and *Penicillium* species (*3*) show a range of subunit size and quaternary structure, but all contain one FAD per monomer. Although the *Penicillium* oxidase shows a strong preference for reduced glutathione, the other enzymes show a broader specificity for small molecular weight thiols including mercaptoethanol, cysteine, and dithiothreitol (DTT[1]). In addition, the seminal and *Aspergillus* enzymes show an apparently modest activity toward cysteine residues in proteins (*1*, *2*). Despite the potential importance of these observations to the post-translational modification of secreted proteins, little is known about the catalytic mechanism of the flavin-linked sulfhydryl oxidases.

The recent characterization of a homodimeric sulfhydryl oxidase from hen egg white confirms that a redox-active disulfide participates in catalysis by these enzymes (*4*, *5*). Two-electron reduction of the enzyme yields a thiolate to oxidized flavin charge-transfer complex (EH_2^A; Scheme 1) apparently analogous to that found with glutathione reductase and a number of other members of the pyridine nucleotide-linked disulfide oxidoreductase family (Scheme 1; ref *6*). Transfer of reducing equivalents to the flavin with regeneration of the active center disulfide yields a second form of EH_2, EH_2^B, and a further 2-electron reduction of this equilibrium mixture generates EH_4 (*6*).

Scheme 1

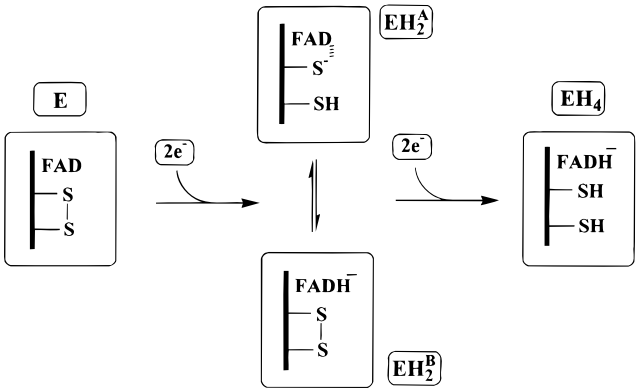

While the evolutionary relationship between the oxidase and the pyridine nucleotide-dependent disulfide oxidoreductases is unclear, the latter provide an invaluable perspective on the likely catalytic strategies employed by the egg white oxidase. Glutathione reductase, for example, catalyzes the reduction of oxidized glutathione by NADPH (*6*−*8*):

$$NADPH + H^+ + GS{-}SG \rightleftharpoons NADP^+ + 2\,GSH$$

NADPH first reduces the flavin moiety of the reductase to generate a species analogous to EH_2^B in Scheme 1. Very rapid internal equilibration yields EH_2^A in which the thiolate of CYS63 (numbering for human enzyme) is the charge-

† This work was supported in part from NIH Grant GM26643 (C.T.).

* To whom correspondence should be addressed. E-mail: cthorpe@udel.edu. Phone: 302-831-2689. Fax: 302-831-6335.

[1] Abbreviations: DTNB, 5,5′-dithio-bis(2-nitrobenzoic acid); DTT, reduced dithiothreitol; GdHCl, guanidine hydrochloride; GSH, reduced glutathione; RNase, pancreatic ribonuclease A.

10.1021/bi9820816 CCC: $18.00
Published on Web 02/19/1999

Scheme 2

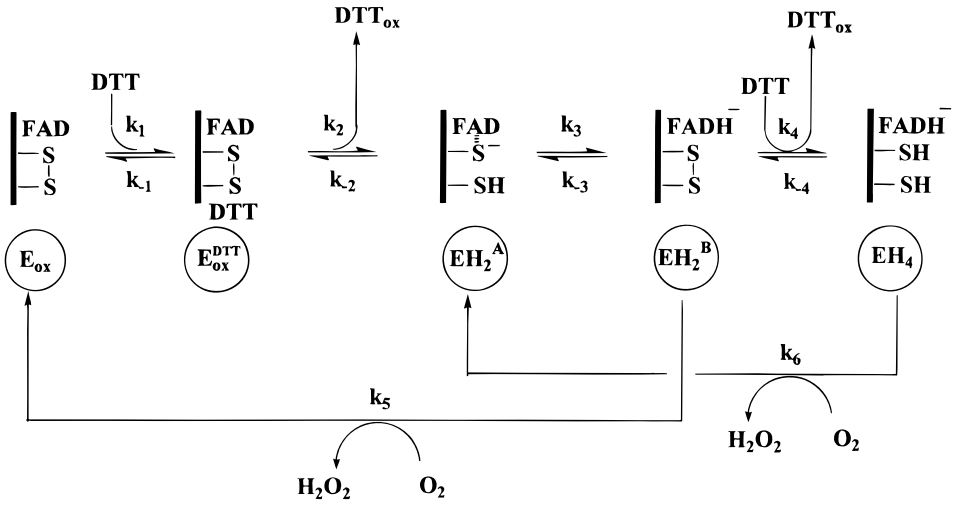

transfer donor to the now-oxidized isoalloxazine ring (*6*−*8*). The other redox-active cysteine residue (CYS58) initiates the oxidative half-reaction by attacking GS−SG (*6*−*8*). Two-electron reduced glutathione reductase shows only a very low reactivity toward molecular oxygen (*9, 10*).

In sulfhydryl oxidase, the flow of reducing equivalents is in reverse. The oxidase is reduced by a suitable thiol substrate to generate EH_2^A (*5*). Subsequent transfer of reducing equivalents to the flavin allows EH_2^B to be oxidized by molecular oxygen in a reaction typical of a flavoprotein oxidase. Presumably the enzyme has evolved to ensure that the hydrogen peroxide generated in this reaction (*1*−*3, 5*) does not adversely affect catalysis. Unlike the extensively studied pyridine nucleotide−disulfide oxidoreductases, the sulfhydryl oxidases cannot communicate with pyridine nucleotides such as NADH and NADPH (*1, 2, 5*).

The present studies have used rapid reaction techniques to investigate the mechanism of the flavoprotein sulfhydryl oxidase from egg white. In view of the limited amount of enzyme available (5000 eggs were used to obtain sufficient protein for these studies), experiments were aimed at defining major features of catalysis. Three representative thiol substrates have been selected. The first, dithiothreitol (DTT), is the best artificial substrate of the enzyme known to date (*5*). The low redox potential of DTT simplifies data analysis because it is an essentially stoichiometric reductant of the oxidase (*5*). Glutathione was studied because of its abundance in many cell types (*11, 12*). Finally, the activity of the egg white enzyme toward reduced RNase as a model protein substrate was examined.

These experiments highlight the major aspects of sulfhydryl oxidase turnover and identify the rate-limiting step common to catalysis with all three substrates. Finally, this work shows that the oxidase is a surprisingly facile catalyst for the oxidation of reduced RNase. Thus, the oxidase may play an important role in the introduction of disulfide bridges in egg white proteins.

MATERIALS AND METHODS

Materials. Sulfhydryl oxidase was isolated and purified from the whites of 5000 eggs of an *rdrd* strain of single comb White Leghorn chickens as described previously (*5*). DTT, GSH, DTNB, RNase, glucose, and glucose oxidase were purchased from Sigma. Desalting columns (PD-10) containing Sephadex G-25 gel were purchased from Pharmacia Biotech.

General Methods. Unless stated otherwise, all buffers were 100 mM potassium phosphate, pH 7.5, and contained 0.3 mM EDTA. Visible and ultraviolet spectra were recorded on a Hewlett-Packard 8452A diode array spectrophotometer. Concentrations of sulfhydryl oxidase were expressed using a molar extinction coefficient of 12.5 mM^{-1} cm^{-1} at 454 nm for the enzyme-bound flavin (*5*). The thiol reagents were standardized before use with DTNB (*13*). Stock solutions of GSH were adjusted to pH 7.5 before use. Standard assays were performed using an oxygen electrode as described previously (*5*). The linearity of these oxygen consumption traces (*5*) suggests that sulfhydryl oxidase is not significantly inhibited by hydrogen peroxide over the time required for the measurements. Furthermore, there is insignificant non-enzymatic reaction of DTT with hydrogen peroxide over this time scale (*5*).

Stopped-Flow Spectrophotometry. Reactions were followed at 4 °C in a kinetic instruments stopped-flow spectrophotometer equipped with a 2 cm path length cell using peripherals and software from Online Instruments Systems. General anaerobic procedures were as described previously (*14*). In reductive experiments with DTT or GSH, a solution of substrate and enzyme were prepared in standard phosphate buffer containing 5 mM glucose. After extensive deoxygenation, 20 nM glucose oxidase was added to the tonometers, followed by two further cycles of evacuation and flushing with nitrogen.

Preparation of EH_4 was by photoreduction of the oxidase in phosphate buffer containing 3 mM EDTA, 1.2 μM deazaflavin (*5, 15*), and 5 mM glucose. Before final flushing of the tonometer, 1 nM glucose oxidase was added. Enzyme was mixed with buffer containing a range of oxygen concentrations prepared as described earlier (*16*). Steady-state kinetic analysis was carried out by enzyme-monitored turnover techniques in the stopped flow as described previously (*17, 18*). In all stopped-flow experiments concentrations are quoted after mixing.

Simulation of the Mechanism Shown in Scheme 2. At present, several of the rate constants in Scheme 2 cannot be determined experimentally (see later). Simulations were

Table 1: Kinetic Constants for Turnover of Egg White Sulfhydryl Oxidase with DTT[a]

k_{-1}/k_1	4.3 mM
k_2	502/s
k_3	3.3/s
k_{-3}	5.7/s
k_6	9×10^5 M^{-1} s^{-1}

[a] Rate constants refer to Scheme 2. Rate constants k_{-2}, k_4, k_{-4}, and k_5 are discussed in the text.

therefore useful in formulating the mechanism and for setting the magnitudes of those rate constants that are currently inaccessible. Scheme 2 was simulated by an iterative routine written in Quick Basic that plots the concentration of each species (or the absorbance of the mixture at 454 or 560 nm) with time. Typically, a time increment of 10^{-6} s was used. The results were checked to ensure that mass balance was retained and that equilibria were correctly predicted. In addition to the rate constants listed in Table 1, the following values were used: k_{-2}, 5/s (DTT is a stoichiometric reductant of the oxidase); k_4, 10^5 M^{-1} s^{-1}; k_{-4}, 10^3 M^{-1} s^{-1}; k_5 varied from 10^3 to 10^7 M^{-1} s^{-1}.

Preparation of Reduced RNase A. Reduced RNase A was obtained by dissolving protein (20 mg) in 1 mL of 100 mM Tris buffer containing 6 M GdHCl adjusted to pH 8 with KOH. A 25-fold excess of DTT over protein thiols was added, and the container was flushed with nitrogen before incubating for 1 h at 37 °C. The mixture was adjusted to pH 3.5 with glacial acetic acid and gel-filtered on a Sephadex G25 (PD10) column equilibrated with deoxygenated 0.1% acetic acid containing 3 mM EDTA. RNase was collected in several fractions and characterized by protein and free thiol content (averaging 7.1 cysteines per molecule). Two methods were used to test that all DTT was removed from reduced RNase upon gel filtration: samples were dialyzed versus 0.1% acetic acid or gel-filtered a second time as above. In all cases the thiol content of RNase was unchanged.

Reduced RNase as a Substrate of Sulfhydryl Oxidase. Freshly prepared reduced RNase was added to give final concentrations of 2.5−45 μM protein in 100 mM air-saturated phosphate buffer, 20 °C, adjusted to pH 7.5 containing 0.1% potassium acetate and 1 mM EDTA. The decline in thiol titer after the addition of 100 nM oxidase was compared with matched controls in the absence of enzyme by diluting aliquots into 6 M GdHCl containing 100 mM Tris/chloride, pH 7.5, and 0.5 mM DTNB (*13*). RNase activity was measured as described previously (*19*).

RESULTS AND DISCUSSION

Turnover of DTT by Egg White Sulfhydryl Oxidase. Scheme 2 is introduced here as a simplified minimal model for the oxidation of DTT by the egg white enzyme. Since the protonation states of thiol and reduced flavin in EH_2 and EH_4 species are not yet known, those depicted in Scheme 2 are for illustrative purposes. These choices do not affect the analysis developed. In the reductive half-reaction, DTT binding generates a Michaelis complex (E_{ox}DTT; k_1/k_{-1}), which reacts via disulfide exchange to yield the charge-transfer species EH_2^A. Internal transfer of two reducing equivalents from the redox-active cysteine pair to the FAD (via k_3, Scheme 2) generates EH_2^B. This 2-electron reduced flavin intermediate can either participate directly in the oxidative phase of catalysis via $k_5[O_2]$, with the regeneration

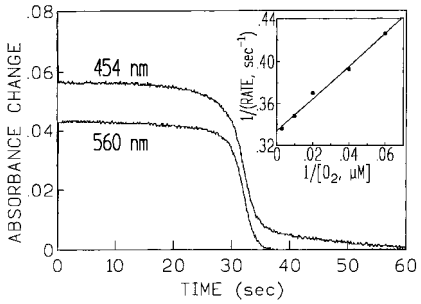

FIGURE 1: Steady-state turnover of egg white sulfhydryl oxidase using DTT as reductant. The oxidase was mixed with DTT in the stopped-flow spectrophotometer to give final concentrations of 3.9 μM enzyme, 0.49 mM DTT, and 0.24 mM oxygen in 100 mM phosphate buffer, pH 7.5, 4 °C. Absorbance changes were monitored at 454 and 560 nm as described in Methods. The inset is a double-reciprocal plot of the turnover numbers extrapolated to infinite DTT concentration versus oxygen concentration. In these experiments DTT concentrations ranged from 0.49 to 4.95 mM.

of E_{ox} and the formation of hydrogen peroxide, or undergo reduction with a second molecule of DTT to form EH_4. The competition between steps k_4[DTT] and $k_5[O_2]$ for EH_2^B determines the extent to which the 4-electron reduced enzyme is catalytically significant. This paper identifies the internal redox equilibration step k_3/k_{-3} as rate-determining in overall turnover with DTT. This sluggish step complicates resolution of the question of the catalytic significance of EH_4 (see later). Since there is little information about the second reductive step with DTT, it is depicted as a simple bimolecular reaction (k_4/k_{-4}, Scheme 2).

Because DTT is a stoichiometric reductant of the oxidase at both E_{ox} and EH_2 levels (*5*), the back reactions k_{-2} and k_{-4} in Scheme 2 can be effectively ignored in this work. The fact that DTT is a dithiol will tend to minimize the concentration of mixed disulfide intermediate between DTT and the oxidase (*12*, *20*).

Enzyme-Monitored Steady-State Turnover Experiments with DTT. Figure 1 shows the absorbance changes at 454 and 560 nm on mixing the enzyme in the stopped-flow spectrophotometer with an excess of DTT in the presence of limiting dissolved oxygen. All rapid reaction kinetic experiments were performed at 4 °C, rather than 25 °C, to facilitate data analysis and to maximize the chances of resolving catalytic intermediates. In Figure 1, the 560 nm absorbance, characteristic of the 2-electron reduced form of the enzyme, increases rapidly and then remains almost constant for over 20 s (Figure 1). Correspondingly, the oxidized flavin absorbance undergoes a rapid partial bleaching before attainment of the steady state.

Since the steady state was maintained for 20 s under these conditions, it could be monitored after manually mixing excess DTT with an aerobic solution of the oxidase in a conventional diode array spectrophotometer (Figure 2). The steady-state spectrum (curve 2) resembles that of the thiolate to oxidized flavin charge-transfer complex obtained in reductive titrations of the oxidase with dithionite, DTT, or glutathione (*5*). However, the long wavelength transition observed in the steady state is approximately 2-fold more intense than that obtained experimentally during anaerobic static titrations (*5*). This is because k_3 (Scheme 2) is rate-limiting in turnover, and enzyme species to the right of this step are rapidly reconverted back to EH_2^A via $k_5[O_2]$ and/or $k_6[O_2]$ followed by steps k_1 and k_2 (see later).

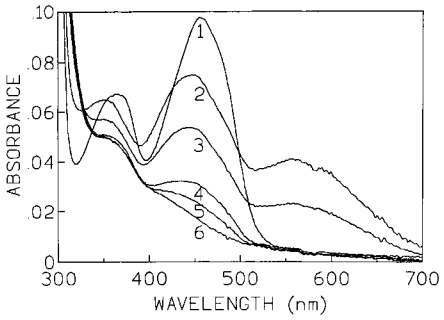

FIGURE 2: Spectrum of sulfhydryl oxidase during turnover in the presence of DTT and oxygen. The oxidase (7.8 μM in 0.8 mL of 100 mM phosphate buffer containing 240 μM dissolved oxygen) was cooled without stirring to 4 °C and the spectrum recorded in a conventional diode array spectrophotometer before (curve 1) and 7, 25, 27, 31, and 107 s after the addition of a total of 5 mM DTT (curves 2−6, respectively). Curve 2 is maintained practically unchanged for 20 s after mixing.

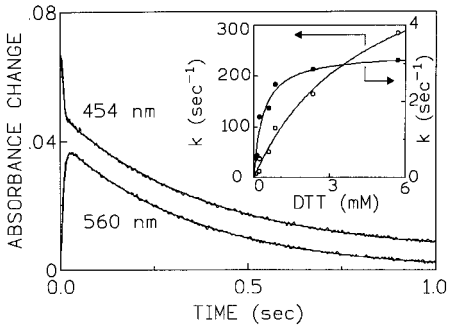

FIGURE 3: Anaerobic reduction of sulfhydryl oxidase by DTT followed by stopped-flow spectrophotometry. The oxidase and DTT were mixed anaerobically (see Methods) in 100 mM phosphate buffer, pH 7.5, to final concentrations of 3.85 μM and 2.39 mM. Both solutions contained 20 nM glucose oxidase and 5 mM glucose to remove traces of oxygen prior to mixing. Absorbance traces at 454 and 560 nm are shown and the smooth lines are fits to two sequential exponentials of 180/s and 2.6/s (454 nm) and 150/s and 2.8/s (560 nm). The inset plots the rate constants for fast (open circles) and slow (solid circles) at 560 nm. Rate constants measured at 454 nm for each DTT concentration are comparable (see the Text). Curves are nonlinear least-squares fits to the data: limit 502/s with an apparent K_d of 4.3 mM DTT and 3.3/s and 0.37 mM for fast and slow phases, respectively.

In Figure 1, the 560 nm absorbance declines rapidly to 0 at about 36 s upon depletion of oxygen. However, full reduction of the oxidized flavin takes approximately 100 s (454 nm trace, Figure 1). This reproducible effect is also seen clearly in Figure 2. Curve 4 (27 s) shows undetectable 560 nm absorbance, yet the bleaching at 454 nm to yield curve 6 requires 107 s. This additional reduction is too slow to be catalytically significant (it is about 20-fold slower than overall turnover with DTT, see later), and cannot be explained by any features of Scheme 2. Conceivably this effect might reflect a small proportion of oxidase without a competent redox-active disulfide. Whatever its origins, this slight apparent heterogeneity does not compromise any of the conclusions developed later.

The 560 nm stopped-flow traces such as that shown in Figure 1 allow the steady-state kinetics to be determined as described earlier (*17, 18*). Experiments with a range of DTT and oxygen concentrations yield a series of parallel lines in double-reciprocal plots. Replots of these data (e.g., inset of Figure 1) yield a maximal turnover number of 3.0/s extrapolated to infinite DTT and oxygen concentration, a K_m value for oxygen at infinite DTT of 4.6 μM, and a K_m for DTT at infinite oxygen of 0.25 mM. The low micromolar K_m for oxygen is consistent with the previously reported upper limit of 20 μM at pH 7.5 and 25 °C suggested by the linearity of oxygen electrode traces when assays are followed to completion (*5*). These steady-state data are consistent with a ping-pong mechanism for the oxidation of DTT as depicted in Scheme 2. Although the observation of apparently parallel lines does not rule out a ternary complex mechanism, there is no obvious chemical reason a ternary mechanism would be required for this flavoprotein.

Anaerobic Reduction of Sulfhydryl Oxidase using DTT. The enzyme-monitored turnover data described above show that EH_2^A predominates in the steady-state when DTT is the reductant. We next examined the reductive half of catalysis under anaerobic conditions. Figure 3 shows representative traces and fits for the reduction of the oxidized enzyme by 2.39 mM DTT at pH 7.5, 4 °C. A rapid increase at 560 nm (150/s), reflecting the formation of EH_2^A in Scheme 2, is followed by a slower decline as EH_4 accumulates (2.8/s). The 454 nm trace is fit to comparable rate constants of 180 and 2.6/s. Examination of reduction at several additional wavelengths from 700 to 300 nm gave no evidence for any spectrally observable intermediates other than E_{ox}, EH_2^A, and EH_4. The slow third reductive phase mentioned in the turnover experiments in Figures 1 and 2 is not seen in the short time scale of Figure 3. Rate constants for this third phase were linearly dependent on DTT concentration (0.16/s at 5.7 mM with an amplitude of 18% of the total change at 454 nm). A value of 0.16/s is some 5% of the overall turnover number determined under these conditions (Figure 1), and so this third phase is not considered further here.

The dependence of the first two phases on DTT concentration is shown in the inset to Figure 3. Only the pseudo first-order rate constants for the 560 nm absorbance changes are plotted, but the 454 nm data are comparable. The fast phase (open circles) yielding EH_2^A is fit to a limiting value of 502/s and a K_d of 4.3 mM. The rate of reduction of lipoamide dehydrogenase by dihydrolipoamide showed corresponding values of 833/s and 0.147 mM at pH 6.2 (*21*). Since DTT is an essentially stoichiometric reductant of the oxidase (*5*) the limiting rate of the fast phase is dominated by the forward rate constant k_2.

The slower second phase leading to the decrease in the charge-transfer band and the accumulation of EH_4 is fit to a saturating rate of 3.3/s with an apparent K_d of 0.37 mM DTT (inset Figure 3, closed symbols). This value is ascribed to the forward rate constant, k_3, for the surprisingly slow internal redox equilibration step between the two forms of EH_2 (Scheme 2). Once the reducing equivalents have been transferred to the flavin, the reformed active site disulfide can be reduced by a second molecule of DTT (via k_4, Scheme 2).

Two factors complicate the characterization of this second reductive step leading to EH_4. First, both EH_2^B and EH_4 are likely to have very similar spectra dominated by the reduced flavin chromophore (*6*). Second, EH_2^B cannot be prepared in isolation without formation of an equilibrium level of the corresponding charge-transfer form, EH_2^A, together with lesser amounts of the disproportionation products E_{ox} and EH_4. This makes interpretation of stopped-flow experiments

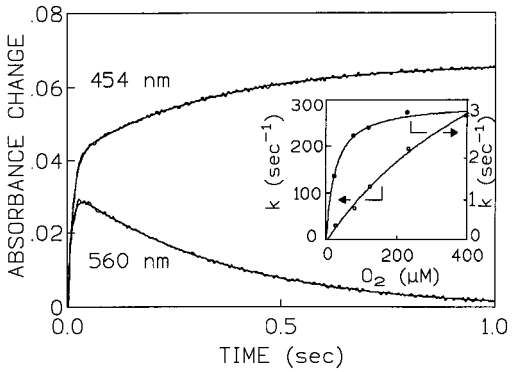

FIGURE 4: Reoxidation of EH_4 by molecular oxygen. Sulfhydryl oxidase in 100 mM phosphate buffer, pH 7.5, containing 1 nM glucose oxidase and 5 mM glucose was photoreduced in a tonometer with 1.2 μM deazaflavin as described in Methods. The fully reduced enzyme was mixed with aerobic phosphate buffer to give final concentrations of 3.1 μM EH_4 and 120 μM oxygen. Absorbance traces at 454 and 560 nm are fit to fast phases of 85/s and 103/s and slow phases of 3.1/s and 2.8/s, respectively. The experiment was repeated from 23 to 398 μM oxygen concentration, and the oxygen dependences of the rate constants measured at 560 nm are shown in the inset. The limiting rate of the slow phase is 3.4/s.

difficult. Although currently inaccessible experimentally, the second reduction step must be faster than about 100/s at 5 mM DTT to make k_3 cleanly rate-determining in the accumulation of EH_4.

The equilibrium constant for the internal redox step (k_3/k_{-3}; Scheme 2) was estimated as 0.58 as follows. Dithionite, photochemical, and DTT equilibrium titration experiments all yield the same extrapolated apparent extinction coefficient of 3.1 mM^{-1} cm^{-1} at 560 nm for EH_2 (EH_2^A + EH_2^B; ref *5*). Since the formation of EH_2^A in the stopped-flow experiments of Figures 1−3 is so much faster than its decay, we assume that the intense charge-transfer band observed in Figures 2 and 3 (ϵ_{app} = 4.9 mM^{-1} cm^{-1}) reflects full formation of this species. For perspective, the thiolate-to-flavin charge-transfer band observed in Figure 2 is of comparable intensity to the most strongly absorbing bands in other flavin-dependent disulfide oxidoreductase. Making the reasonable assumption that EH_2^B does not itself absorb significantly at 560 nm (*6*, *22*) allows calculation of the internal equilibrium constant:

$$[EH_2^B]/[EH_2^A] = (4.9\ mM^{-1}\ cm^{-1} - 3.1\ mM^{-1}\ cm^{-1})/3.1\ mM^{-1}\ cm^{-1}$$

Thus, redox equilibration at the EH_2 level is sluggish (see later) in the egg white oxidase. The forward step, k_3, of 3.3/s appears almost entirely rate-limiting during turnover of DTT (maximal turnover number 3.0/s under the same conditions). Step k_3 also intervenes in the reoxidation of the 4-electron reduced enzyme by molecular oxygen as described in the next section.

Reoxidation of 4-Electron Reduced Oxidase by Molecular Oxygen. EH_4 was prepared by catalytic photoreduction at pH 7.5 (see Methods) and mixed at 4 °C with various concentrations of dissolved oxygen in the stopped-flow instrument. Figure 4 shows traces for a final concentration of 120 μM oxygen. The charge-transfer intermediate followed at 560 nm appears rapidly (103/s) and decays much more slowly (2.8/s). Similarly the absorbance increases at 454 nm are strongly biphasic with comparable rate constants (85/s and 3.1/s). Examination of this reaction at a range of other wavelengths showed no evidence for additional intermediates other than EH_4, EH_2, and E_{ox} species. The dependences of both fast and slow phases on the oxygen concentration are shown in the inset to Figure 4. The rapid phase (open circles) shows an approximately linear response up to at least 200 μM oxygen, and these data has been used to estimate a bimolecular rate constant of 9×10^5 M^{-1} s^{-1} for k_6.

In sharp contrast, the slower phase saturates at a rate of 3.4/s, essentially the same value as observed during reduction of the oxidase with DTT. Scheme 2 provides an explanation for the interaction between oxygen and EH_4. The slow step (k_3) intervenes between the two oxygen-dependent steps (k_6 and k_5) and therefore limits this second oxidative step. For this reason k_5 cannot be estimated directly from these data. As noted previously, the fact that k_3 limits the rate of reappearance of E_{ox} suggests that k_5 is rapid. Indeed it might be expected that both EH_4 and EH_2^B might have similar bimolecular rate constants for their reaction with dioxygen since both contain dihydroflavin (Scheme 2).

A simulation of the reoxidation of EH_4 as described in Materials and Methods, varying k_5 from 10^3 to 10^8 M^{-1} s^{-1}, shows that this rate constant must be at least 10^6 M^{-1} s^{-1} to yield the data in Figure 4. The absorbance changes at 454 nm are particularly informative. Rate constants for k_5 below 10^6 M^{-1} s^{-1} lead to a noticeable dip in the absorbance at the end of the fast phase. This dip reflects the extent to which the internal equilibrium between EH_2^A and EH_2^B is established in the face of competing reoxidation of EH_2^B via k_5 (Scheme 2). We have deferred attempts to measure k_5 directly because of the complexities in data analysis and the scarcity of pure enzyme.

Scheme 2 as a Model for Catalysis. Table 1 lists equilibrium and rate constants obtained for turnover with DTT. DTT binds relatively weakly to the oxidase (K_d 4.3 mM) but subsequent reduction is rapid (502/s). As mentioned earlier, k_3 severely limits catalysis with DTT. Further, the similarity of maximal turnover numbers for a wide range of thiol substrates (ref *5*; from β-mercaptoethanol to reduced RNase; see later) suggests that this step is largely limiting in all of these instances. After transfer of reducing equivalents to the flavin, EH_2^B partitions between reoxidation via k_5 or further reduction via k_4. Clearly, the distribution between these two processes will depend on the relative concentrations of DTT and oxygen, but it would not be expected to seriously affect overall turnover because this is governed almost exclusively by k_3.

Reduction of Sulfhydryl Oxidase by Reduced Glutathione. GSH is an abundant thiol in many eukaryotic cells (*11*, *12*) and must therefore be considered as a potential substrate of the egg white oxidase (*5*). Static titrations of the egg white oxidase show that, unlike the stoichiometric reductant DTT, approximately 7 and 100 equivalents of GSH are required to attain maximal EH_2 and EH_4 states, respectively (*5*). These data are consistent with redox potential measurements for free GSH and DTT ($E^{\circ\prime}$ of −0.24 vs −0.31 V; ref *6*, *12*). Figure 5 plots rate constants for the formation and disappearance of this species as a function of GSH concentration. Kinetically, GSH is a markedly poorer reductant than DTT; for example, comparing 4 mM dithiol DTT with 8 mM monothiol GSH yields observed rates for the appearance of

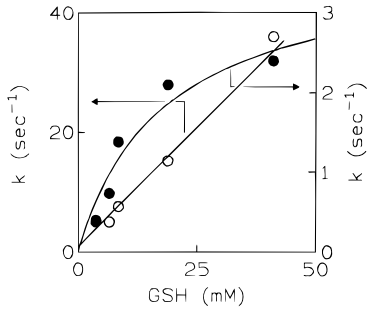

FIGURE 5: Reduction of sulfhydryl oxidase by glutathione. The conditions were those of Figure 3 using GSH as a substrate. Rate constants measured at 454 and 560 nm for fast (open circles) and slow phases (closed circles) are plotted as a function of GSH concentration. The slow phase is fit to a limiting rate of 3.6/s with an apparent K_d of 18 mM. A linear fit to the fast phase is shown.

EH_2^A (the fast phase) of 236/s and 7/s, respectively. This fast phase with GSH shows no evidence for saturation up to 40 mM thiol (Figure 5, open circles). The corresponding slow phase with GSH (apparent K_d of 18 mM) shows a limiting rate of 3.6/s at 4 °C in good agreement with the value of k_3 determined earlier with DTT (3.3/s) and with reoxidation of EH_4 with molecular oxygen (3.4/s). These rapid reaction studies with GSH show, at least qualitatively, why DTT exhibits a much lower K_m than GSH in steady-state turnover (*5*). Thus the comparatively facile reduction of the enzyme by DTT makes k_3 rate-determining at much lower concentrations than those required for GSH (Scheme 2).

Reduced RNase as a Substrate of Egg White Sulfhydryl Oxidase. Earlier studies showed that both the rat seminal vesicle and the *Aspergillus* enzymes were modestly active toward reduced RNase as a model substrate for disulfide bond formation in proteins (see later). Because preliminary work suggested that the egg white enzyme was an effective oxidant of reduced RNase (H. G. Gilbert, unpublished observation), we have kinetically examined RNase as a third substrate of sulfhydryl oxidase. Reduced RNase was prepared by reduction with DTT under denaturing conditions and freed of excess DTT by gel filtration (see Methods). In preliminary experiments, the reduced RNase was gel-filtered a second time or dialyzed to make certain that traces of DTT were not mediating the interaction between oxidase and protein substrate. No change in thiol content of RNase was observed after this second step. Thus the disulfide bond formation described below reflects a direct communication between the oxidase and reduced RNase.

The oxidase was incubated with reduced RNase at 20 °C, and aliquots were removed for thiol content determinations using DTNB (see Methods). The reduced RNase preparation contained on average 7.1 free thiols out of an expected eight, and this declined rapidly in air-saturated buffer in the presence of 114 nM sulfhydryl oxidase (Figure 6). The inset plot shows that the initial rates can be fit to a maximal turnover number of 850 disulfide bonds formed/min and an apparent K_m of 70 μM/protein thiol (10 μM for reduced RNase).

Thus pancreatic RNase is an excellent substrate of the egg white oxidase with a k_{cat}/K_m about 1.4×10^6 M^{-1} s^{-1} at 20 °C (see later). Rapid reoxidation of RNase does not result in a substantial regain in enzymatic activity; under conditions similar to those shown in Figure 6 (94 nM oxidase and 35 μM reduced RNase), complete reoxidation of protein thiols

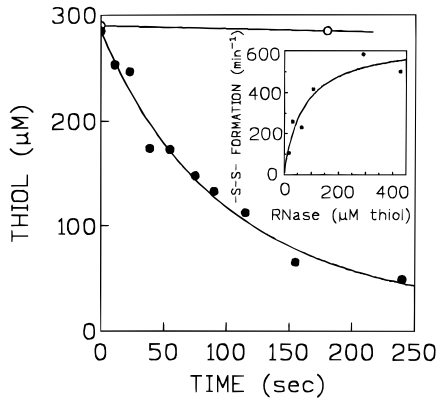

FIGURE 6: Oxidation of reduced RNase by egg white oxidase. Reduced RNase (see Methods) was diluted to 45 μM in 100 mM phosphate buffer pH 7.5, 20 °C, containing 240 μM oxygen, and aliquots were removed for the measurement of thiol content (see Experimental Procedures) in the absence (open circles) or presence (solid circles) of 114 nM oxidase. The experiment was repeated over a range of RNase concentrations. Initial rates for the first 30 s were corrected for the small background contribution in the absence of oxidase and plotted as a function of RNase concentration in the inset. The solid line is a nonlinear least-squares fit to a maximal turnover of 850/s and a K_m of 70 μM RNase thiols (10 μM reduced RNase).

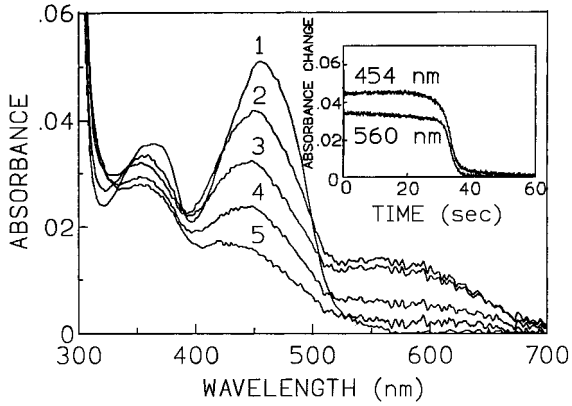

FIGURE 7: Spectrum of sulfhydryl oxidase during turnover of reduced RNase under aerobic conditions. The spectrum of the oxidase was recorded before (curve 1) and 14, 22, 30, and 100 s after the addition of a reduced RNase (see Methods). Final concentrations were 4.1 μM oxidase, 100 μM RNase, and approximately 240 μM dissolved oxygen at 4 °C in 100 mM phosphate buffer pH 7.5. The inset shows absorbance changes after mixing the oxidase in the stopped-flow spectrophotometer with RNase at 4 °C to give final concentrations of 3.9 and 175 μM, respectively.

regenerates only 10% of the RNase activity (see Methods).

Figure 7 (curve 2) shows the steady-state spectrum of the enzyme introducing disulfide bridges into reduced RNase at 4 °C. The inset shows the time course of these spectral changes followed in the stopped flow at 560 and 454 nm (but using 175 μM instead of 100 μM RNase). The results are qualitatively similar to those observed with DTT (Figure 1), although the slow phase seems less evident because reduction does not proceed to quite the same extent (compare Figure 2, curve 6, with Figure 7 curve 5). Nevertheless, reduced RNase is a surprisingly effective thermodynamic and kinetic reductant of the oxidase.

Conclusions. In this study, a range of experiments was chosen to identify key aspects of the mechanism of this rather scarce enzyme. This work provides a satisfactory explanation for the similarity in the maximal turnover numbers for a

range of thiol substrates of the enzyme. Thus, the internal step k_3, involving reduction of the FAD by the active site dithiol, strongly limits turnover at high substrate concentrations. This step (about 3.3/s at 4 °C) is slow compared to values of greater than 800/s for lipoamide dehydrogenase (*6*, *23*, *24*), 110/s for glutathione reductase (*7*), and 23/s for *Escherichia coli* thioredoxin reductase (*25*). It is not clear whether this sluggishness reflects an intrinsically slow chemical step or a structural rearrangement prior to the redox reaction. The crystal structure of thioredoxin reductase from *E. coli*, for example (*25*, *26*), suggests that a domain rotation brings NADPH in contact with the isoalloxazine ring while simultaneously breaking redox communication between flavin and the disulfide. It should be noted that the intensity of the charge-transfer complex in Figure 2 is certainly consistent with close proximity between thiolate donor and flavin acceptor. There is currently no evidence for the accumulation of a C-4a adduct (*6*) during any of the experiments of this study.

This work shows that the egg white oxidase is a facile, but apparently random, oxidant of the cysteine residues in reduced RNase from bovine pancreas. Comparison of k_{cat}/K_m for GSH, DTT, and RNase (expressed in terms of their molar concentration without regard to variable thiol contents) gives values of 1.2×10^3, 1.2×10^5, and 1.4×10^6 M^{-1} s^{-1}, respectively. On a per-thiol basis, these values become 1.2×10^3, 6×10^4, and 1.8×10^5 M^{-1} s^{-1} for GSH, DTT, and RNase, respectively. By either measure, RNase thiols are much better substrates of sulfhydryl oxidase than is glutathione.

A plausible role of the egg white oxidase is as a direct participant in disulfide bond formation during passage of secreted proteins through the endoplasmic reticulum (*27*−*31*). This aspect of the protein folding problem is still poorly understood (*32*−*36*). One suggestion for the immediate oxidant for disulfide bond formation was cystamine formed by a microsomal flavoprotein hydroxylase that oxidizes cysteamine at the expense of NADPH and molecular oxygen (*32*). Oxidized glutathione, selectively transported into the lumen of the endoplasmic reticulum (*33*), has been widely believed to represent a primary oxidant for disulfide bond formation. However, recent evidence suggests that oxidized glutathione is not necessary for disulfide bond formation in yeast (*34*). Finally, genetic screens have recently identified a novel redox-active protein (ERO1) in yeast that is closely involved in disulfide bond formation (*34*−*36*). Its precise role in the oxidative functions of the endoplasmic reticulum will become clear with an understanding of its enzymatic activities (*34*, *35*).

Since the facile oxidation of a pancreatic RNase by an egg white sulfhydryl oxidase may not be representative of secreted proteins in general, future studies will examine whether reduced denatured egg white proteins are substrates of the oxidase. In addition, the effects of protein disulfide isomerase on the outcome of sulfhydryl oxidase incubations needs investigation.

ACKNOWLEDGMENT

We thank Harold White and Hiram Gilbert for stimulating discussions and Robert Alphin for maintaining the flock of chickens at the University of Delaware farm. The helpful comments of a reviewer are gratefully acknowledged.

REFERENCES

1. Ostrowski, M. C., and Kistler, W. S. (1980) *Biochemistry 19*, 2639−2645.
2. de la Motte, R. S., and Wagner, F. W. (1987) *Biochemistry 26*, 7363−7371.
3. Kusakabe, H., Kuninaka, A., and Yoshino, A. (1982) *Agric. Biol. Chem. 46*, 2057−2067.
4. de la Motte, R. S., and Wagner, F. W. (1987) *Fed. Proc. 46*, 3529.
5. Hoober, K. L., Joneja, B., White, H. B., III, and Thorpe, C. (1996) *J. Biol. Chem. 271*, 30510−30516.
6. Williams, C. H., Jr. (1992) in *Chemistry and Biochemistry of Flavoenzymes* (Müller, F., Ed.) Vol. III, pp 121−211, CRC Press, Boca Raton, FL.
7. Rietveld, P., Arscott, L. D., Berry, A., Scrutton, N. S., Deonarain, M. P., Perham, R. N., and Williams, C. H., Jr. (1994) *Biochemistry 33*, 13888−13895.
8. Karplus, P. A., and Schulz, G. E. (1987) *J. Mol. Biol. 95*, 701−729.
9. Williams, C. H., Jr. (1976) *Enzymes* (3rd ed.) *13*, 89−173.
10. Arscott, L. D., Drake, D. M., and Williams, C. H., Jr. (1989) *Biochemistry 28*, 3591−3598.
11. Meister, A. (1995) *Methods Enzymol. 251*, 3−7.
12. Gilbert, H. F. (1995) *Methods Enzymol. 251*, 8−28.
13. Ellman, G. L. (1959) *Arch. Biochem. Biophys. 82*, 70−77.
14. Lehman, T. C., and Thorpe, C. (1990) *Biochemistry 29*, 10594−10602.
15. Massey, V., and Hemmerich, P. (1978) *Biochemistry 17*, 9−17.
16. DuPlessis, E. R., Pellet, J., Stankovich, M. T., and Thorpe, C. (1998) *Biochemistry 37*, 10469−10477.
17. Chance, B. J. (1943) *J. Biol. Chem. 151*, 553−577.
18. Gibson, Q. H., Swoboda, B. E. P., and Massey, V. J. (1964) *J. Biol. Chem. 239*, 3927−3934.
19. Bergmeyer, H. (1983) in *Methods of Enzymatic Analysis* (Bergmeyer, H., Ed.) Vol. III, pp 306−307, Verlag Chemie, Basel, Switzerland.
20. Creighton, T. E. (1984) *Methods Enzymol. 107*, 305−329.
21. Matthews, R. G., Ballou, D. P., Thorpe, C., and Williams, C. H., Jr. (1977) *J. Biol. Chem. 252*, 3199−3207.
22. Wilkinson, K. D., and Williams, C. H., Jr. (1979) *J. Biol. Chem. 254*, 851−862.
23. Massey, V., Gibson, Q. H., and Veeger, C. (1960) *Biochem. J. 77*, 341−351.
24. Benen, J., van Berkel, W., Dieteren, N., Arscott, L. D., Williams, C. H., Jr., Veeger, C., and de Kok, A. (1992) *Eur. J. Biochem. 207*, 487−497.
25. Lennon, B. W., and Williams, C. H., Jr. (1997) *Biochemistry 36*, 9464−9477.
26. Waksman, G., Krishna, T. S. R., Williams, C. H., Jr., and Kuriyan, J. (1994) *J. Mol. Biol. 236*, 800−816.
27. Helenius, A., Marquardt, T., and Braakman, I. (1992) *Trends Cell Biol. 2*, 227−231.
28. Chen, W., Helenius, J., Braakman, I., and Helenius, A. (1995) *Proc. Natl. Acad. Sci. U.S.A. 92*, 6229−6233.
29. Gilbert, H. F. (1997) *J. Biol. Chem. 272*, 29399−29402.
30. Freedman, R. B., Dunn, A. D., and Ruddock, L. W. (1998) *Curr. Biol. 8*, 468−470.
31. Bardwell, J. C. A., and Beckwith, J. (1993) *Cell 74*, 769−771.
32. Ziegler, D. M., and Poulsen, L. L. (1977) *Trends Biochem. Sci. 2*, 79−81.
33. Hwang, C., Sinskey, A. J., and Lodish, H. F. (1992) *Science 257*, 1496−1502.
34. Frand, A. R., and Kaiser, C. A. (1998) *Mol. Cell 1*, 161−170.
35. Pollard, M. G., Travers. K. J., and Weissman, J. S. (1998) *Mol. Cell 1*, 171−182.
36. Freedman, R. B., Dunn, A. D., and Ruddock, L. W. (1998) *Curr. Biol. 8*, R468−R470.

BI9820816